Articles

Syntheses, X-ray Powder Structures, and Preliminary Ion-Exchange Properties of Germanium-Substituted Titanosilicate Pharmacosiderites: $HM_3(AO)_4(BO_4)_3 \cdot 4H_2O$ (M = K, Rb, Cs; A = Ti, Ge; B = Si, Ge)

Elizabeth A. Behrens, Damodara M. Poojary,† and Abraham Clearfield*

Received January 14, 1997. Revised Manuscript Received December 30, 1997

This paper describes a continuing research effort that involves synthesizing new tunnel-type materials while attempting to understand their fundamental ion-exchange selectivities through the process of structural elucidation. For this study, we hydrothermally synthesized and characterized two germanium-substituted titanosilicates in the cesium phase and prepared their potassium forms by ion exchange. A mixed Si//Ti/Ge_phase, $HCs_3(TiO)_{3.5}(GeO)_{0.5}(GeO_4)_{2.5}(SiO_4)_{0.5} \cdot 4H_2O$, crystallizes in the cubic space group $P\bar{4}3m$ with $a = 7.9376(1)$ Å, while the cesium titanogermanate, $HCs_3(TiO)_4(GeO_4)_3 \cdot 4H_2O$, possesses a body-centered supercell belonging to space group $I23$, $a = 15.9604(3)$ Å. Differences in symmetry between the two cesium compounds can be explained in terms of entropy and site mixing in the Si/Ti/Ge compound. Upon ion exchange with potassium, the resulting phases, $HK_3(TiO)_{3.5}(GeO)_{0.5}(GeO_4)_{2.5}(SiO_4)_{0.5} \cdot 4H_2O$ and $HK_3(TiO)_4(GeO_4)_3 \cdot 4H_2O$, distorted to the tetragonal space group $P4b2$, with $a = b = 11.1571(2)$, $c = 7.9165(2)$ Å, and $a = b = 11.215(1)$, $c = 7.9705(2)$ Å, respectively. For the first time, we have observed tetragonal distortions with alkali cation forms of the pharmacosiderite analogues. As compared to $HK_3(TiO)_4(SiO_4)_3 \cdot 4H_2O$, these potassium germanium-substituted phases show remarkable increases in strontium and cesium selectivity, which proves very beneficial for nuclear waste remediation applications. An increase in selectivity can be explained in terms of their inherent structures and bond strengths associated with the charge-neutralizing cations and framework oxygens.

Introduction

We recently reported on the syntheses, crystal structures, and ion-exchange properties for a series of titanosilicates with the general formula $HM_3(TiO)_4(SiO_4)_3 \cdot 4{-}8H_2O$ ($M = H^+, K^+, Cs^+$).[1,2] These compounds were prepared as part of an ongoing research program to understand the relationship between structure and ion-exchange selectivity for tunnel-type ion exchangers.[3,4]

The previously published structures are isostructural with the mineral pharmacosiderite.[1] Pharmacosiderite is a naturally occurring mineral whose framework composition is $[(FeOH)_4(AsO_4)_3]^-$ and crystallizes in a primitive cubic unit cell that belongs to the $P\bar{4}3m$ symmetry space group with $a = 7.98$ Å. Alternating Fe octahedra and As tetrahdera create a three-dimensional tunnel structure where each cube face is composed of metal ions that form eight-membered rings with charge-balancing cations and water molecules residing in the channels.[5]

Limited work has been conducted on the structural characterization of the titanosilicate pharmacosiderites and their ion-exchanged phases;[1,2,6,7] however, there is a growing interest toward the germanate analogues, $HM_3Ge_7O_{16} \cdot 4{-}6H_2O$ ($M = Na^+, K^+, Rb^+, Cs^+$), because of their attractive zeolitic properties such as ion exchange and reversible dehydration.[8−10] For example, Feng et al. investigated a series of dehydrated germanates, $HM_3Ge_7O_{16} \cdot 4{-}6H_2O$ ($M = Li^+, NH_4+, Na^+, K^+, Rb^+, Cs^+$), which possessed better ionic conductivity than traditional zeolites.[8−10] Nevertheless, the ion-exchange behavior for these germanates was not explored.

* To whom correspondence should be addressed.
† Currently with Symyx Technologies, Santa Clara, CA 95051.

(1) Behrens, E. A.; Poojary, D. M.; Clearfield., A. *Chem. Mater.* **1996**, *8*, 1236.
(2) Behrens, E. A.; Clearfield, A. *Microporous Mater.* **1997**, *11*, 65.
(3) Poojary, D. M.; Bortun, A. I.; Bortun, L. N.; Clearfield, A. *Inorg. Chem.* **1996**, *35*, 6131. Poojary, D. M.; Bortun, A. I.; Bortun, L. N.; Clearfield, A. *Inorg. Chem.* **1997**, *36*, 3072.
(4) Poojary, D. M.; Cahill, R. A.; Clearfield, A. *Chem. Mater.* **1994**, *6*, 2364.
(5) Zemann, J. *Tscherm. Miner. Petr. Mitt.* **1948**, *1*, 121; *Acta Crystallogr.* **1959**, *12*, 252.
(6) Chapman, D. M.; Roe, A. L. *Zeolites* **1990**, *10*, 730.
(7) Harrison, W. T. A.; Gier, T.; Stucky, G. D. *Zeolites* **1995**, *15*, 408.
(8) Feng, S.; Greenblatt, M. *Chem. Mater.* **1992**, *4*, 462.
(9) Feng, S.; Tsai, S.; Greenblatt, M. *Chem. Mater.* **1992**, *4*, 468.
(10) Feng, S.; Tsai, M.; Greenblatt, M. *Chem. Mater.* **1992**, *4*, 388.

S0897-4756(97)00037-9 CCC: $15.00
Published on Web 03/10/1998

Another interesting aspect of the germanate pharmacosiderite analogues is their ability to undergo structural distortion which is contingent upon the degree of dehydration and the nature of the charge-balancing cation. Previous studies showed that most of the pharmacosiderite-type compounds retain their cubic space group symmetry, $P\bar{4}3m$, when exchanged with different monovalent charge-neutralizing cations.[11,12] Several papers by Roberts and Fitch[13−15] also presented extensive structural characterization by Rietveld analysis using powder synchrotron and neutron diffraction data for the series of compounds $M_{4-x}H_xGe_7O_{16}\cdot nH_2O$ (M represents any monovalent cation). The fully hydrated potassium, cesium, and rubidium germanates were described as body-centered superstructures ($I23$) where the lattice parameters increased in accordance with the size of the cation.[15] Upon partial dehydration, the cesium and rubidium phases revert back to their original parent symmetry, $P\bar{4}3m$, while the potassium form changes symmetry to a $2 \times 2 \times 2$ face-centered cubic supercell ($F23$). Concurrently, Nenoff et al.[16] prepared a rhombohedrally distorted hydrogen phosphate-containing germanium pharmacosiderite with the general formula $Na_3H_x(H_2PO_4)_x[Ge_7O_{16}]\cdot 4H_2O$. This compound exhibits both cation- and anion-exchange capabilities and transforms from rhombohedral to cubic symmetry ($P\bar{4}3m$) after ion exchange with monovalent or divalent cations.

Our original research interest was focused on the titanosilicate pharmacosiderites as potential cesium and strontium exchangers for nuclear waste and ground water remediation applications. We found that the potassium titanosilicate pharmacosiderite selectively exchanged strontium in neutral to slightly basic solutions that contained high concentrations (5−6 M) of sodium admixed with a variety of other cations.[2] Neither the potassium, proton, nor sodium forms efficiently removed cesium from similar solutions. One explanation for this low selectivity was attributed to a size mismatch between the pore openings and cesium cations. Due to space constraints within the tunnels, the cesium cations could not reside exactly in the face centers at their ideal positions (0, $^1/_2$, $^1/_2$), ($^1/_2$, 0, $^1/_2$), and ($^1/_2$, $^1/_2$, 0). Instead, they are displaced to either side of their ideal sites where the cesium cations form four long (3.408(2) Å) and four short (3.143(3) Å) bonds with the silicate oxygens. A more thermodynamically stable environment would occur if the pore was slightly larger in order to accommodate the cesium ions into the face center positions where they could ideally form eight equal Cs−O bonds at 3.25 Å.

One way to achieve this goal is by isomorphously substituting larger metal ions into the framework (e.g., Zr for Ti or Ge for Si). An earlier report[17] suggested that one could judiciously synthesize pharmacosiderite exchangers with different metal ions in the framework, which in turn, changes the unit cell dimensions and hence their respective pore diameters. Another example resides in the mineral sodium titanosilicate, which has a similar arrangement of edge-sharing TiO_6 clusters, but also contains minor amounts of Nb and smaller amounts of Zr and Fe in the titanium sites.[18]

For this study, we altered the tetrahedral and some octahedral positions by substituting different amounts of Ge for Si. Two cesium compounds, $HCs_3(TiO)_{3.5}(GeO)_{0.5}(GeO_4)_{2.5}(SiO_4)_{0.5}\cdot 4H_2O$ and $HCs_3(TiO)_4(GeO_4)_3\cdot 4H_2O$, were prepared hydrothermally and then treated with KCl to produce their respective potassium forms, $HK_3(TiO)_{3.5}(GeO)_{0.5}(GeO_4)_{2.5}(SiO_4)_{0.5}\cdot 4H_2O$ and $HK_3(TiO)_4(GeO_4)_3\cdot 4H_2O$. These four samples were characterized by powder X-ray diffraction and Rietveld methods in order to fully understand the crystal symmetry and, more importantly, the bonding environments around the cesium and potassium cations. Like the pure, fully hydrated germanates, the titanogermanate compound $HCs_3(TiO)_4(GeO_4)_3\cdot 4H_2O$ crystallizes in a body centered ($I23$) supercell, and for the first time, we have observed tetragonal distortions in the pharmacosiderite structures when cesium cations were exchanged with potassium. We also report on preliminary ion-exchange data for the four phases and relate structural data with the observed ion-exchange selectivity.

Experimental Section

Materials and Methods. Reagent-grade chemicals were obtained from commercial sources and used without further purification. Thermogravimetric analyses (TGA) were performed on a Dupont model no. 910 unit at a heating rate of 10 °C/min under N_2 atmosphere. X-ray powder patterns were gathered on a Rigaku RU-200 automated powder diffractometer with Cu Kα radiation. Germanium, titanium, and silicon analyses were obtained from Galbraith Laboratories Inc. (Knoxville, TN).

Synthesis of the Cesium Ge−Substituted Titanosilicate, $HCs_3(TiO)_{3.5}(GeO)_{0.5}(GeO_4)_{2.5}(SiO_4)_{0.5}\cdot 4H_2O$. The partially Ge-substituted pharmacosiderite was prepared by mixing 1.831 g (6.3 mmol) of titanium isopropoxide (97%, Aldrich), 0.375 g (6.3 mmol) of fumed silica (99.7%, Sigma), and 10 mL of distilled deionized (ddi) water to form a white gel. The gel was stirred overnight after which it was centrifuged, the supernatant discarded, and an additional 3 mL of ddi water was added. A separate cesium germanate solution was prepared by combining 0.673 g (6.4 mmol) of GeO_2 (99.999%, STREM) with 23.54 g (79 mmol) of CsOH (50 wt %, Aldrich). The cesium germanate solution was then poured into the gel, and the final mixture was heated in a 100 mL Teflon-lined steel vessel at 200 °C for 48 h. The final product was filtered, washed with ddi water, and dried at 60 °C (final mass: 1.51 g). Analytical data observed: Ge, 19.37%; Ti, 14.53%; Si, 1.89%; H_2O loss up to 800 °C, 4.42%. Calculated: Ge, 19.33%; Ti, 14.87%; Si, 1.25%; H_2O, 6.39%.

Synthesis of the Cesium Ge−Substituted Titanosilicate, $HCs_3(TiO)_4(GeO_4)_3\cdot 4H_2O$. Complete Ge-substitution for Si was accomplished by entirely replacing GeO_2 for fumed silica in the above synthetic preparation. 1.770 g (6.0 mmol) of titanium isopropoxide was mixed with 6.6 mL of ddi water to form a white gel. A separate cesium germanate solution was prepared by mixing 1.884 g (18.0 mmol) of GeO_2 and 38.3 g (127 mmol) of CsOH. The two different mixtures were

(11) Schmetzer, K.; Horn, W.; Bank, H. *N. Jb. Miner. Mh.* **1981**, *3*, 97.
(12) Walenta, K. *Tscherm. Miner. Petr. Mitt.* **1966**, *11*, 121.
(13) Roberts, M. A.; Fitch, A. N. *J. Phys. Chem. Solids* **1991**, *52*, 1209.
(14) Roberts, M. A.; Fitch, A. N.; Chadwick, A. V. *J. Phys. Chem. Solids* **1995**, *56*, 1353.
(15) Roberts, M. A.; Fitch, A. N. *Z. Kristallogr.* **1996**, *211*, 378.
(16) Nenoff, T. M.; Harrison, W. T. A.; Stucky, G. D. *Chem. Mater.* **1994**, *6*, 525.
(17) Chapman, D. M. *Crystalline Group IVA Metal-Containing Molecular Sieve Compositions*; U.S. Patent 5,015,453, 1991.
(18) Sokolova, E. V.; Ratsvetaeva, R. K.; Andrianov, V. I.; Egorov-Tismenko, Y. K.; Men'shikov, Y. P. *Dokl. Akad. Nauk. SSSR* **1989**, *307*, 114.

combined and stirred to thoroughly homogenize, and the gel was then reacted in a 100 mL Teflon-lined steel vessel at 200 °C for 48 h. The product was filtered, washed with ddi water, and dried at 60 °C (final mass: 1.13 g). Analytical data observed: Ge, 20.18%; Ti, 15.41%; H_2O up to 800 °C, 6.93%. Calculated: Ge, 19.16%; Ti, 16.84%; H_2O, 6.33%. It is important to note that the pharmacosiderite phases are typically prepared with excess SiO_2 or GeO_2. We showed in a previous paper[1] that the K and Cs phases of titanosilicate pharmacosiderite were prepared by using an approximate 1:2 molar ratio for Ti:Si. Chapman and Roe[6,18] also adopted a similar molar ratio for the preparation of their titanosilicate pharmacosiderite phases. Most likely the excess Si or Ge remains in solution after hydrothermal treatment, but it is also possible to expect minor amounts of Si and Ge present as an amorphous phase.

Preparation of Potassium Phases of Ge−Substituted Compounds $HK_3(TiO)_{3.5}(GeO)_{0.5}(GeO_4)_{2.5}(SiO_4)_{0.5}\cdot 4H_2O$ and $HK_3(TiO)_4(GeO_4)_3\cdot 4H_2O$. Since pure and highly crystalline potassium phases could not be prepared directly by the use of KOH, the potassium phases reported here were obtained by ion exchange of the previously prepared Cs phases. The Cs phases (partially and fully substituted titanosilicates) were treated with 3 M KCl, and the ion-exchange reaction was carried out between 60 and 80 °C for 8 h. These reactions were repeated a total of three times for each sample to ensure complete potassium exchange. The products were filtered, washed, and dried at 60 °C. Elemental analysis of the solid indicated that most of the cesium ions were exchanged for potassium. For example, the observed %K for KTiSiGe was 11.95% (calculated 13.8%).

Distribution Coefficients. Ion-exchange measurements were carried out under batch conditions using 1×10^{-3} M alkali and alkaline earth cation stock solutions, which were prepared from their respective metal chloride salts dissolved in ddi water. A typical procedure entailed mixing a certain mass of exchanger and volume of metal stock solution to give a final volume-to-solid ratio of 200 ml:1 g. Samples were shaken for 24 h at ambient temperature after which the samples were filtered using Whatman #1 or #42 filter paper. Initial and final cation concentrations were analyzed with atomic absorption or emission (AA/AE) spectroscopy using a Varian model A-250 spectrometer. Final pHs of each filtrate were measured using an Orion SA-720 pH meter. Distribution coefficients (K_ds) were calculated using eq 1

$$K_d = \left(\frac{C_o}{C_f} - 1\right)\left(\frac{V}{m}\right) = \frac{\text{ml}}{\text{g}}$$

where C_o and C_f are the original and final equilibrium concentrations of the metal ions in solution, respectively, V is the total volume of stock solution, and m is the mass of exchanger.

X-ray Data Collection, Structure Solution, and Rietveld Refinement. Step-scanned X-ray powder diffraction data (side-loaded into a flat aluminum sample holder) were collected for the finely ground samples. The X-ray source was a Rigaku rotating anode generator operating at 50 kV and 180 mA with a copper target and graphite monochromator. A 0.5° divergence and scatter slits together with a 0.15° receiving slit were employed for data collection. Using a Rigaku-controlled diffractometer, the data were collected using a 0.01° step size in the 2θ range 10−100° and a count time between 6 and 10 s/step. The $K\alpha_2$ contribution was mathematically removed from the data sets, and peak picking was conducted as described earlier. Each pattern was indexed by Ito methods[19] on the basis of the first 20 observed reflections in the profile. Sample $HCs_3(TiO)_{3.5}(GeO)_{0.5}(GeO_4)_{2.5}(SiO_4)_{0.5}\cdot 4H_2O$ was found to have the same space group symmetry, $P\bar{4}3m$, as the parent iron arsenate mineral[20] with a unit cell dimension around a = 7.94 Å. In the case of the cesium titanium germanate, $HCs_3(TiO)_4(GeO_4)_3\cdot 4H_2O$, the unit cell dimensions doubled to a give a body-centered supercell with a = 15.96 Å. Systematic absences for this data set indicated that the space group was either $I\bar{4}3m$ or $I23$. The original cubic symmetry for the two cesium phases was lowered to tetragonal symmetry, $P\bar{4}b2$, when cesium cations were replaced by potassium. Initial unit cell dimensions were found to be $a = b$ = 11.22 and c = 7.97 Å for $HK_3(TiO)_4(GeO_4)_3\cdot 4H_2O$ and $a = b$ = 11.16 and c = 7.92 Å for $HK_3(TiO)_{3.5}(GeO)_{0.5}(GeO_4)_{2.5}(SiO_4)_{0.5}\cdot 4H_2O$.

Rietveld refinement[21] for $HCs_3(TiO)_{3.5}(GeO)_{0.5}(GeO_4)_{2.5}(SiO_4)_{0.5}\cdot 4H_2O$ was based upon atomic positional parameters for the proton titanosilicate. Similarly, initial structural models for space group symmetries $I\bar{4}3m$, $I23$, and $P\bar{4}b2$ were obtained by transforming the same atomic positions in accordance with symmetry requirements and known framework structures. $HCs_3(TiO)_4(GeO_4)_3\cdot 4H_2O$ was refined in both space groups $I\bar{4}3m$ and $I23$. Final agreement factors for the refinement were very similar in both space groups, but the cesium cation positions were more stable in the noncentric space group $I23$. Roberts and Fitch also reported on a series of pure germanate pharmacosiderite phases whose structures were described as $I23$ symmetry.[15] Rietveld refinement for all four powder patterns were carried out with the program GSAS.[21] After the initial refinements, such as scale factor, background functions, lattice parameters, zero point errors, and profile coefficients, difference Fourier maps were computed, which revealed water oxygen and charge-neutralizing cation (K and Cs) positions.

The cesium cation was disordered over two positions about its ideal position, thus it was refined with 50% occupancy. Each structure was refined with soft constraints for tetrahedral Si−O or Ge−O bond distances and O−O nonbonded distances. Si−O and Ge−O bonds were constrained to 1.63(2) and 1.75(2) Å, respectively. Similar constraints were obtained on the bond angles by holding the O−O nonbonded distances at 2.64(2) Å for Si and 2.85(2) Å for Ge tetrahedra. The initial weight (factor = 200) of these constraints was reduced as the refinement progressed, but they could not be completely removed without some structural distortions. Final cycles of the refinement produced weight factors around 50. Lattice water molecules and charge-balancing cations were refined without any geometrical constraints. All atoms were refined isotropically, and neutral atomic scattering factors were used.[22] There were no corrections for absorption or preferred orientation.

Crystallographic data are given in Table 1, final positional and thermal parameters in Tables 2−5, and selected bond lengths and angles are presented in Tables 6−9. Final Rietveld difference plots are shown in Figures 1−4.

Results

The compounds presented in this study are isostructural with the natural mineral pharmacosiderite. However, symmetry changes for compounds $HCs_3(TiO)_{3.5}(GeO)_{0.5}(GeO_4)_{2.5}(SiO_4)_{0.5}\cdot 4H_2O$, $HCs_3(TiO)_4(GeO_4)_3\cdot 4H_2O$, $HK_3(TiO)_{3.5}(GeO)_{0.5}(GeO_4)_{2.5}(SiO_4)_{0.5}\cdot 4H_2O$, and $HK_3(TiO)_4(GeO_4)_3\cdot 4H_2O$ resulted in different positional parameters (Tables 2−5). The framework structure for $HCs_3(TiO)_{3.5}(GeO)_{0.5}(GeO_4)_{2.5}(SiO_4)_{0.5}\cdot 4H_2O$ belongs to space group $P\bar{4}3m$ which is built from titanium−oxygen, silicon−oxygen, and germanium−oxygen polyhedra. Generally, 12.5% of the octahedral Ti sites and around 83.3% of the tetrahedral Si positions were replaced by

(19) Visser, J. *Appl. Crystallogr.* **1969**, *2*, 89.
(20) Buerger, M. J.; Dollase, W. A.; Garaycochea-Wittke, I. *Z. Kristallogr.* **1967**, *125*, 92.
(21) Larson, A.; von Dreele, R. B. *GSAS: Generalized Structure Analysis System, LANSCE*; Los Alamos National Laboratory, Copyright 1985−1988 by the Regents of the University of California.
(22) Cromer, D. T.; Waber, J. T. *International Tables for X-ray Crystallography*; Kynoch Press: Birmingham, U.K., 1974; Vol. IV, Table 2.2A (distributed through Kluwer Academic Publishers, Dordrecht).

Table 1. Crystallographic Parameters for the Different Pharmacosiderite Phases[a]

	CsTiSiGe	CsTiGe	KTiSiGe	KTiGe
pattern range (2θ), deg	10−85	10−90	10−100	10−100
space group	$P\bar{4}3m$ (no. 215)	123 (no. 197)	$P\bar{4}b2$ (no. 117)	$P\bar{4}b2$ (no. 117)
a (Å)	7.9376(1)	15.9606(3)	11.1571(2)	11.215(1)
c (Å)			7.9165(2)	7.9705(2)
V (Å^3)	500.12	4065.8	985.4	1002.51
Z	1	8	2	2
no. of reflections	55	279	303	308
expected R_{wp}[b]	0.035	0.035	0.040	0.036
R_{wp}[c]	0.143	0.140	0.105	0.083
R_p[c]	0.101	0.105	0.080	0.066
R_F[c]	0.058	0.060	0.047	0.051

[a] Formulas: CsTiSiGe = $HCs_3(TiO)_{3.5}(GeO)_{0.5}(GeO_4)_{2.5}(SiO_4)_{0.5}\cdot 4H_2O$. CsTiGe = $HCs_3(TiO)_4(GeO_4)_3\cdot 4H_2O$. KTiSiGe = $HK_3(TiO)_{3.5}(GeO)_{0.5}(GeO_4)_{2.5}(SiO_4)_{0.5}\cdot 4H_2O$. KTiGe = $HK_3(TiO)_4(GeO_4)_3\cdot 4H_2O$. [b] Expected $R_{wp} = R_{wp}/(\chi^2)^{1/2}\chi^2 = \sum w(I_o - I_c)^2/(N_{obs} - N_{var})$. [c] $R_{wp} = (\sum w(I_o - I_c)^2/\sum[wI_o^2])^{1/2}$; $R_p = (\sum|I_o - I_c|/\sum I_c)$; $R_F = \langle|F_o| - |F_c|\rangle/\langle|F_o|\rangle$.

Table 2. Positional and Thermal Parameters for $HCs_3(TiO)_4(GeO_4)_3\cdot 4H_2O$[a]

	x	y	z	U_{iso}, Å^2
Ti1[b]	0.1844(10)	0.1844(10)	0.1844(10)	0.015(5)
Ti2	0.1807(8)	0.1781(7)	0.6821(11)	0.015(5)
Ge1	0.0023(11)	0.2469(7)	0.2562(5)	0.011(10)
O11	0.1986(11)	0.3103(14)	0.1878(13)	0.048(16)
O12[b]	0.1860(17)	0.1860(17)	0.8140(17)	0.048
O21	−0.0620(12)	0.1862(18)	0.3164(16)	0.048
O22	−0.0597(15)	0.3178(14)	0.1963(11)	0.048
O23	0.0686(21)	0.3107(15)	0.3182(15)	0.048
O24	0.0613(13)	0.1885(11)	0.1858(11)	0.048
O31[c]	0	0	0	0.048
O32	0.4020(20)	0.4368(15)	0.9155(26)	0.048
Cs1[d]	0.1925(10)	0.5	0	0.027(6)
Cs2[d]	0.2421(5)	0.5	0	0.018(4)
Cs3[d]	0.2239(17)	0	0	0.022(6)
Cs4[d]	0.2839(18)	0	0	0.021(5)

[a] Occupancies of Cs atoms are about 50%. O31, O32 represent water oxygen atoms. [b] Site symmetry: 3. [c] Site symmetry: 23. [d] Site symmetry: 2.

Table 3. Positional and Thermal Parameters for $HK_3(TiO)_4(GeO_4)_3\cdot 4H_2O$

	x	y	z	U_{iso}, Å^2
Ti1	0.1389(2)	−0.0106(3)	0.1445(4)	0.003(8)
Ge1[a]	0.2647(1)	0.2353(1)	0	0.015(7)
Ge2[b]	0	0	0.5	0.014(7)
O1	0.1513(5)	0.2374(6)	−0.1408(6)	0.017(10)
O2	0.2627(6)	0.0961(5)	0.1102(8)	0.017
O3	0.1101(6)	−0.0085(10)	−0.0979(11)	0.017
O4	−0.1244(7)	0.0126(9)	0.3714(8)	0.017
O5[d]	0.3272(8)	−0.0413(8)	0.7498(15)	0.093(8)
K1[a]	0.2831(3)	0.2169(3)	0.5	0.075(3)
K2[c]	0.5	0	0	0.088(5)

[a] Site symmetry: 2. [b] Site symmetry: $\bar{4}$. [c] Site symmetry: 222. [d] O(5) represents water oxygen atom.

Ge atoms. The titanium atoms are octahedrally coordinated and are located on a mirror plane and close to the origin, $\bar{4}3m$, in the crystal. Hence, the $\bar{4}$ symmetry generates a cluster of four titanium atoms bridged together by O2 atoms to form a $(TiO)_4$ cubelike unit similar to that shown in Figure 5a. However, this atomic arrangement creates distorted geometries due to the Ti−O2 bridging atoms. These Ti clusters reside in all eight corners of the unit cell and are linked together by O1 oxygen atoms from silicate (germanate) groups located between clusters at ($^1/_2$, 0, 0). This arrangement of metal−oxygen clusters bridged by silicate (germanate) groups generates a three-dimensional tunnel structure whose pore openings are filled with water molecules and charge-neutralizing cesium cations. A similar Ti arrangement holds for $HCs_3(TiO)_4(SiO_4)_3\cdot 4H_2O$.[1] However, when the germanate ion replaces silicate to form $HCs_3(TiO)_4(GeO_4)_3\cdot 4H_2O$, a change in space group to $I23$ occurs. The lower symmetry requires two independent titanium sites, designated Ti1, a special position on the 3-fold axis, and Ti2, in a general position (Figure 5b). A reduction in symmetry is probably determined by the larger germanate groups. We note that half of the unit cell dimension ($I23$) for the larger unit cell is considerably smaller than would be expected if germanium atoms were substituted for silicon in the $P\bar{4}3m$ unit cell. The lower symmetry allows greater freedom to position the titanium atoms, which results in a conservation of space (approximately 10 vol %).

Table 4. Positional and Thermal Parameters for $HCs_3(TiO)_{3.5}(GeO)_{0.5}(GeO_4)_{2.5}(SiO_4)_{0.5}\cdot 4H_2O$[a]

	x	y	z	U_{iso}, Å^2
Ti1(Ge)[b]	0.1402(4)	0.1402(4)	0.1402(4)	0.020(2)
Ge1(Si)[c]	0.5	0	0	0.005(2)
O1[d]	0.3699(6)	0.1243(3)	0.1243(3)	0.005(2)
O2[b]	0.1161(9)	0.1161(9)	−0.1161(9)	0.004(4)
O(3)[b,f]	0.3614(8)	0.6386(8)	0.3614(8)	0.086(5)
Cs1[e,f]	0.0457(17)	0.5	0.5	0.120(5)

[a] Occupancy refinement of Ti1 [1.07(1)] showed electron density higher than that for a fully occupied pure Ti atom, which indicates random site filling by germanium atoms (87.5% Ti and 12.5% Ge). Similarly, the occupancy of Ge1 was refined to 0.90(1) which accounts for about 83% Ge and 17% Si atoms at this site. [b] Site symmetry: $3m$. [c] Site symmetry: $\bar{4}2m$. [d] Site symmetry: m. [e] Site symmetry: $mm2$. [f] Cs1 is disordered over two sites with 50% occupancy. O(3) represents water oxygen atoms.

Table 5. Positional and Thermal Parameters for $HK_3(TiO)_{3.5}(GeO)_{0.5}(GeO_4)_{2.5}(SiO_4)_{0.5}\cdot 4H_2O$[a]

	x	y	z	U_{iso}, Å^2
Ti(Ge)1	0.1377(2)	−0.0098(2)	0.1393(4)	0.015(3)
Ge(Si)1[b]	0.2658(2)	0.2342(2)	0	0.018(2)
Ge(Si)2[c]	0	0	0.5	0.004(2)
O1	0.1466(5)	0.2348(6)	−0.1353(7)	0.017(4)
O2	0.2627(5)	0.1012(4)	0.1175(7)	0.017
O3	0.1119(6)	−0.0095(7)	−0.1092(10)	0.017
O4	−0.1189(7)	0.0038(7)	0.3789(8)	0.017
O5[e]	0.3208(10)	−0.0404(8)	0.7252(18)	0.094(4)
K1[b]	0.2736(3)	0.2264(3)	0.5	0.110(4)
K2[d]	0.5	0	0	0.096(8)

[a] Occupancy factors for octahedral and tetrahedral sites, as obtained for the mixed cesium compound, were used for structural refinement. The Ti1 site is randomly occupied with approximately 87.5% titanium atoms and 12.5% germanium atoms. Ge1 and Ge2 occupancies add up to 2.5 for the formula, and the remaining 0.5 of the sites are filled by silicon atoms. [b] Site symmetry: 2. [c] Site symmetry: $\bar{4}$. [d] Site symmetry: 222. [e] O(5) represents water oxygen atom.

Table 6. Bond Lengths (Å) and Bond Angles (deg) for $HCs_3(TiO)_4(GeO_4)_3 \cdot 4H_2O$

atoms	distance		atoms	distance	
Ti1−O11	2.02(2)	3×	Ti1−O24	1.97(2)	3×
Ti2−O11	2.16(2)		Ti2−O11	1.94(2)	
Ti2−O12	2.11(2)		Ti2−O21	1.90(2)	
Ti2−O22	1.91(2)		Ti2−O23	1.82(3)	
Ge1−O21	1.71(1)		Ge1−O22	1.78(1)	
Ge1−O23	1.77(1)		Ge1−O24	1.74(1)	
Cs1−O21	3.09(3)	2×	Cs1−O22	3.54(3)	2×
Cs1−O23	3.63(3)	2×	Cs1−O23	3.22(3)	2×
Cs1−O32	3.74(4)	2×	Cs1−O32	2.92(3)	2×
Cs2−O21	3.22(3)	2×	Cs2−O22	3.22(3)	2×
Cs2−O23	3.29(3)	2×	Cs2−O23	3.35(3)	2×
Cs2−O32	3.06(4)	2×	Cs2−O32	3.52(3)	2×
Cs3−O21	3.46(3)	2×	Cs3−O22	3.60(2)	2×
Cs3−O24	3.17(2)	2×	Cs3−O24	3.22(2)	2×
Cs3−O32	3.58(6)	2×	Cs3−O31	3.57(3)	2×
Cs4−O21	3.17(3)	2×	Cs4−O22	3.32(2)	2×
Cs4−O24	3.47(2)	2×	Cs4−O24	3.53(2)	2×
Cs4−O32	2.81(6)	2×			

atoms	angle		atoms	angle	
O11−Ti1−O11	81.9(11)	3×	O11−Ti1−O24	94.5(7)	3×
O11−Ti1−O24	90.7(7)	3×	O11−Ti1−O24	172.2(11)	3×
O24−Ti1−O24	92.5(9)	3×	O11−Ti2−O11	80.4(13)	
O11−Ti2−O12	79.5(10)		O11−Ti2−O21	89.9(11)	
O11−Ti2−O22	166.7(9)		O11−Ti2−O23	94.8(11)	
O11−Ti2−O12	84.7(12)		O11−Ti2−O21	170.0(10)	
O11−Ti1−O22	88.0(9)		O11−Ti2−O23	88.2(2)	
O12−Ti2−O21	91.4(10)		O12−Ti2−O22	93.1(10)	
O12−Ti2−O23	171.5(13)		O21−Ti2−O22	101.4(11)	
O21−Ti2−O23	94.9(12)		O22−Ti2−O23	91.3(12)	
O21−Ge1−O22	109.2(8)		O21−Ge1−O23	111.8(8)	
O21−Ge1−O24	112.7(8)		O22−Ge1−O23	105.4(8)	
O22−Ge1−O24	107.1(7)		O23−Ge1−O24	110.3(8)	

Table 7. Bond Lengths (Å) and Bond Angles (deg) for $HK_3(TiO)_4(GeO_4)_3 \cdot 4H_2O$

atoms	distance		atoms	distance	
Ti1−O1	1.927(6)		Ti1−O2	1.853(5)	
Ti1−O3	1.959(9)		Ti1−O3	2.028(10)	
Ti1−O3	2.026(10)		Ti1−O4	1.816(7)	
Ge1−O1	1.697(4)	2×	Ge1−O2	1.792(4)	2×
Ge2−O4	1.737(6)	4×	K1−O1	3.231(6)	2×
K1−O2	3.397(7)	2×	K1−O4	3.366(7)	2×
K1−O4	3.293(11)	2×	K1−O5	3.548(9)	2×
K1−O5	3.585(14)	2×	K2−O1	3.579(6)	4×
K2−O2	3.003(6)	4×	K2−O5	2.819(13)	4×

atoms	angle		atoms	angle	
O1−Ti1−O2	95.5(3)		O1−Ti1−O3	95.1(4)	
O1−Ti1−O3	90.8(3)		O1−Ti1−O3	163.3(3)	
O1−Ti1−O4	93.2(4)		O2−Ti1−O3	88.3(4)	
O2−Ti1−O3	159.8(4)		O2−Ti1−O3	94.8(4)	
O2−Ti1−O4	102.8(4)		O3−Ti1−O3	72.0(3)	
O3−Ti1−O3	72.1(4)		O3−Ti1−O4	165.4(4)	
O3−Ti1−O3	75.3(3)		O3−Ti1−O4	95.9(9)	
O3−Ti1−O4	97.3(4)		O1−Ge1−O1	114.6(4)	
O1−Ge1−O2	109.2(3)	2×	O1−Ge1−O2	109.1(2)	2×
O2−Ge1−O2	105.2(4)		O4−Ge2−O4	110.4(3)	3×
O4−Ge2−O4	107.7(5)	3×			

The Ti−O1 and Ti−O2 bond lengths (Table 8) for the mixed cesium Si/Ti/Ge compound are 1.832(5) Å and 2.053(4) Å, respectively. The Ti−O2 bonds are significantly longer than Ti−O1 because a proton is most likely bonded to O2. For the cesium titanogermanate, the O1 atoms interconnect TiO_6 octahedra while the O2 atoms link together TiO_6 and GeO_4 groups. As shown in Figure 5b, the cluster of four TiO_6 octahedra are more distorted than in the mixed Si/Ti/Ge (Figure 5a) compound, which generates a wide range of Ti(O1,2)−O1 and Ti(O1,2)−O2 bond lengths (Table 6). Germanate

Table 8. Bond Lengths (Å) and Bond Angles (deg) for $HCs_3(TiO)_{3.5}(GeO)_{0.5}(GeO_4)_{2.5}(SiO_4)_{0.5} \cdot 4H_2O$

atoms	distance		atoms	distance	
Ti1−O1	1.832(5)	3×	Ti1−O2	2.053(4)	3×
Ge1−O1	1.736(4)	4×	Cs1−O1	3.217(3)	4×
Cs1−O1	3.432(6)	4×	Cs1−O3	2.950(11)	2×
Cs1−O3	3.586(12)	2×			

atoms	angle		atoms	angle	
O1−Ti1−O1	97.6(2)	3×	O1−Ti1−O2	91.0(2)	6×
O1−Ti1−O2	166.8(5)	3×	O2−Ti1−O2	78.9(6)	3×
O1−Ge1−O1	110.7(2)	3×	O1−Ge1−O1	107.0(3)	3×

Table 9. Bond Lengths (Å) and Bond Angles (deg) for $HK_3(TiO)_{3.5}(GeO)_{0.5}(GeO_4)_{2.5}(SiO_4)_{0.5} \cdot 4H_2O$

atoms	distance		atoms	distance	
Ti1−O1	1.871(6)		Ti1−O2	1.873(5)	
Ti1−O3	1.988(8)		Ti1−O3	2.013(7)	
Ti1−O3	1.987(8)		Ti1−O4	1.910(7)	
Ge1−O1	1.708(4)	2×	Ge1−O2	1.752(4)	2×
Ge2−O4	1.637(6)	4×	K1−O1	3.218(7)	2×
K1−O2	3.337(6)	2×	K1−O4	3.240(10)	2×
K1−O4	3.379(7)	2×	K1−O5	3.325(15)	2×
K1−O5	3.510(10)	2×	K2−O1	3.546(6)	4×
K2−O2	3.025(6)	4×	K2−O5	2.989(17)	4×

atoms	angle		atoms	angle	
O1−Ti1−O2	96.1(3)		O1−Ti1−O3	93.9(3)	
O1−Ti1−O3	90.5(3)		O1−Ti1−O3	166.4(3)	
O1−Ti1−O4	96.3(3)		O2−Ti1−O3	90.9(3)	
O2−Ti1−O3	166.1(3)		O2−Ti1−O3	94.2(3)	
O2−Ti1−O4	98.6(4)		O3−Ti1−O3	76.5(3)	
O3−Ti1−O3	77.1(3)		O3−Ti1−O4	165.2(3)	
O3−Ti1−O3	77.6(3)		O3−Ti1−O4	92.7(4)	
O3−Ti1−O4	90.9(4)		O1−Ge1−O1	112.8(4)	
O1−Ge1−O2	109.1(3)	2×	O1−Ge1−O2	108.7(2)	2×
O2−Ge1−O2	108.4(2)		O4−Ge2−O4	110.0(3)	3×
O4−Ge2−O4	108.3(5)	3×			

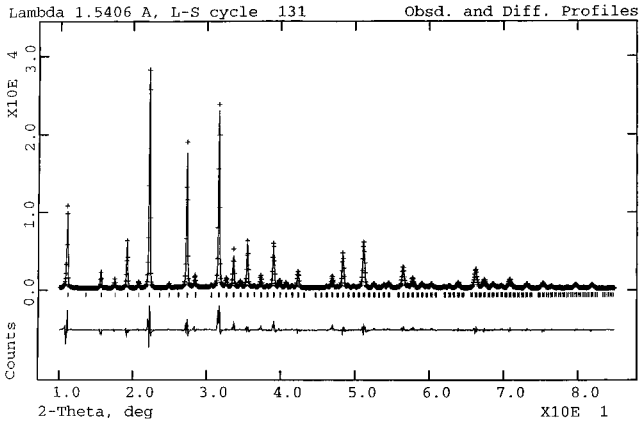

Figure 1. Observed (+) and calculated (−) profiles for the Rietveld refinement of $HCs_3(TiO)_4(GeO_4)_3 \cdot 4H_2O$. The bottom curve is a difference plot on the same intensity scale. Tick marks represent calculated peak positions.

tetrahedra in both structures display very regular bond lengths.

Both $HCs_3(TiO)_4(GeO_4)_3 \cdot 4H_2O$ and $HCs_3(TiO)_{3.5}(GeO)_{0.5}(GeO_4)_{2.5}(SiO_4)_{0.5} \cdot 4H_2O$ possess cesium cations that occupy sites near the unit cell face centers and are disordered over two positions with 50% occupancy. As a result of the superstructure, the cesium titanogermanate contains four independent cesium cations but two different sets of cation positions. Cs1 and Cs2, occupy the sites (x, $^1/_2$, 0) while Cs3 and Cs4 reside at (x, 0, 0). Cs1, Cs2, and Cs3 are essentially 12-coordinate while Cs4 is 10-coordinate, although several of the

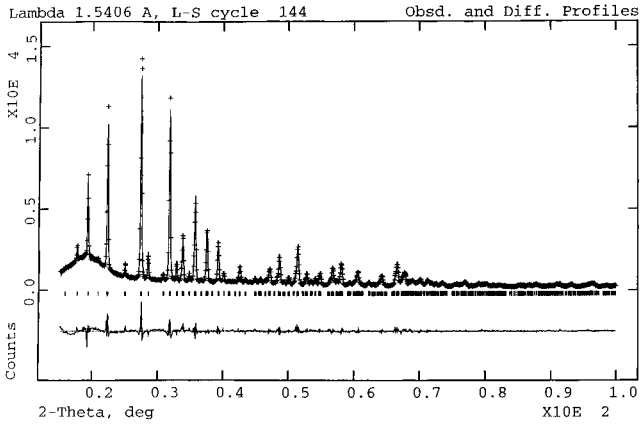

Figure 2. Rietveld plot for $HK_3(TiO)_4(GeO_4)_3 \cdot 4H_2O$.

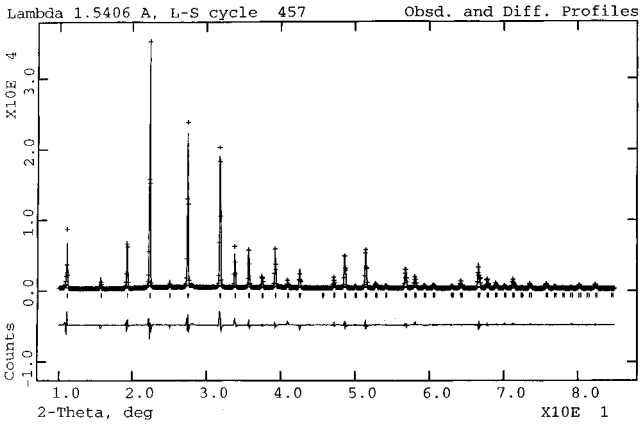

Figure 3. Rietveld plot for $HCs_3(TiO)_{3.5}(GeO)_{0.5}(GeO_4)_{2.5}(SiO_4)_{0.5} \cdot 4H_2O$.

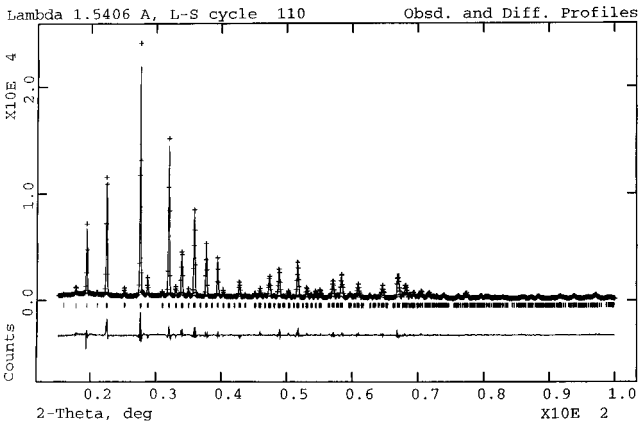

Figure 4. Rietveld plot for $HK_3(TiO)_{3.5}(GeO)_{0.5}(GeO_4)_{2.5}(SiO_4)_{0.5} \cdot 4H_2O$.

distances are larger than the sum of their respective radii. Water oxygen O32 provides four binding sites to Cs1 and Cs2, although two of the Cs1−O32 bonds are relatively longer (3.74 Å) than the others (Table 6). Four water oxygen atoms, O32 and O31, coordinate Cs3 with two sets of bond distances, 3.58(6) and 3.57(3) Å, respectively. Cs4 completes its 10-coordination by forming two relatively short Cs4−O32 bonds at 2.81(6) Å and its symmetry equivalent. On the other hand, the mixed Si/Ge/Ti compound only has one cesium position in which each cation is 12-coordinate with eight binding contacts to the germanate groups, 3.217(3)−3.432(6) Å, and four surrounding water molecules with two long,

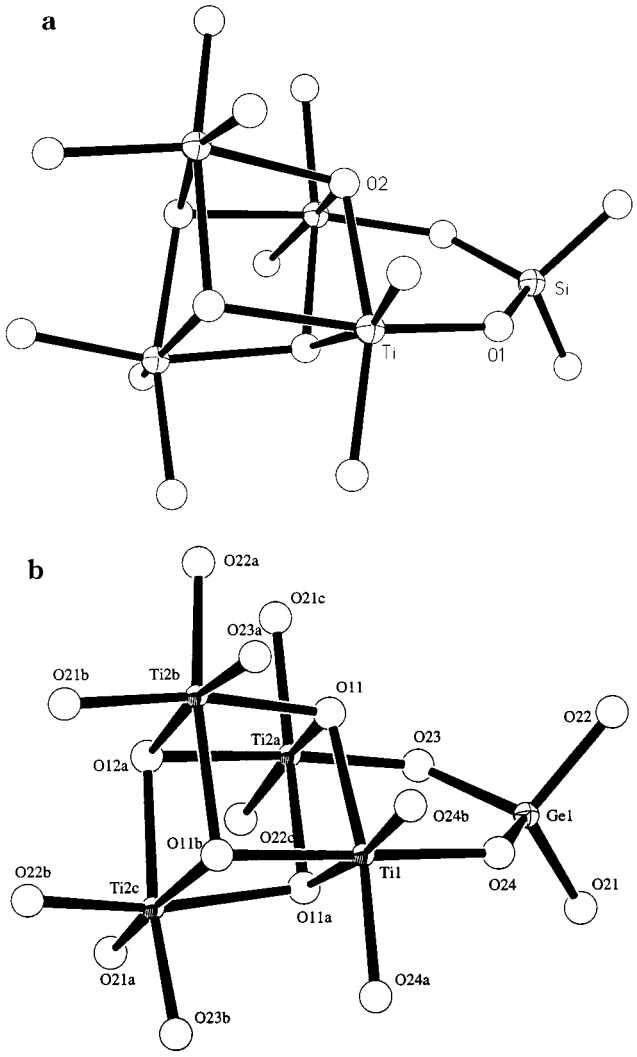

Figure 5. (a) Atomic arrangement for the four titanium octahedra in the $(TiO)_4$ clusters in the structure of $HCs_3(TiO)_{3.5}(GeO)_{0.5}(GeO_4)_{2.5}(SiO_4)_{0.5} \cdot 4H_2O$ (space group $P\bar{4}3m$). (b) Atomic arrangement for the four titanium octahedra in the $(TiO)_4$ clusters in the structure of $HCs_3(TiO)_4(GeO_4)_3 \cdot 4H_2O$ (space group $I23$).

3.586(12) Å, and two short, 2.950(11) Å, bonds (Table 8).

Upon ion exchanging the cesium phases with potassium, their respective geometries reduced in symmetry from cubic to tetragonal. The two potassium phases $HK_3(TiO)_{3.5}(GeO)_{0.5}(GeO_4)_{2.5}(SiO_4)_{0.5} \cdot 4H_2O$ and $HK_3(TiO)_4(GeO_4)_3 \cdot 4H_2O$ belong to the space group $P\bar{4}b2$ where their *a*- and *b*-dimensions correspond to face diagonals of the parent structure. The octahedral Ti and Ge atoms are located on general positions and are bound to four different oxygen atoms with varying bond lengths. As noted in Figure 6, two different types of tetrahedral sites exist in these structures. One site occupies the $\bar{4}$ symmetry position and the other has 2-fold symmetry. The former type of Ge or Si atoms are bound to symmetry-related positions by O4 atoms and the latter to oxygen atoms O1 and O2.

Both potassium phases contain two independent positions for the potassium ions. The first potassium, K1, is located on a 2-fold axis and the other, K2, is at an intersection of three 2-fold axes. The potassium ion K1 is located at $z = {}^1/_2$ between unit-cell-translated Ge1

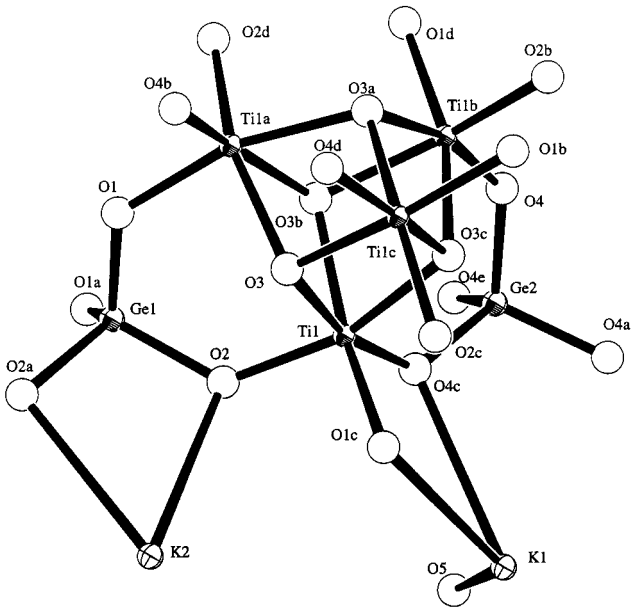

Figure 6. A sectional diagram involving sample $HK_3(TiO)_4(GeO_4)_3 \cdot 4H_2O$ showing the atom labeling and connections involved in linking the titanium octahedra (tetragonal, space group $P\bar{4}b2$).

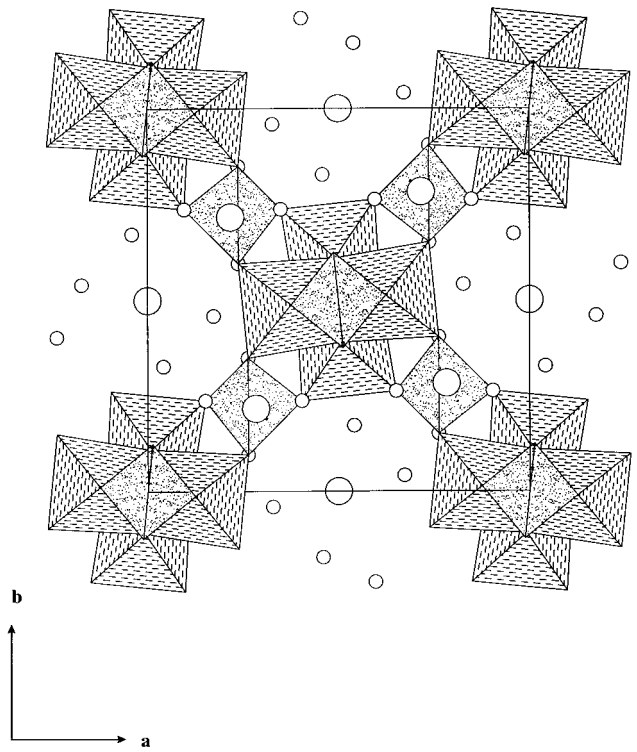

Figure 7. Polyhedral representation for $HK_3(TiO)_4(GeO_4)_3 \cdot 4H_20$ as viewed down the *c*-axis. Coordination of K2 (excluding four long K−O1 bonds) is shown. K1 atoms are located between two K2 atoms along the (110) diagonal direction, and these two atoms are shifted $^1/_2$ along the *c*-axis. K1 is sandwiched between two Ge1 tetrahedra translated 1 unit along the *c*-axis. The striped polyhedra are the TiO_6 octahedra, and the stippled polyhedra represent the GeO_4 tetrahedra. The stippled polyhedra in the center of the $(TiO)_4$ clusters are at (0 0 $^1/_2$) and bridge the cluster in the *z*-direction.

tetrahedra along the *c*-axis. K1 atoms are 8-coordinate and have binding contacts with germanate (silicate) oxygens with relatively long bond distances (Tables 7 and 9). K2 is also 8-coordinate but is located in the *ab*-plane at 0, $^1/_2$, 0 and $^1/_2$, 0, 0 (Figure 7). In general, K2 has four bonds from the germanate (silicate) oxygens (K2−O2) and the other four involve water oxygens (K2−O5). The K2−O1 contacts are probably too long (∼3.5 Å) for stable K−O bonds.

Ion-Exchange Behavior. Batch distribution coefficients (K_ds) and the equilibrium pH values (in parentheses) are given in Table 10 and include values for the pure potassium titanium silicate phase determined earlier.[1] Batch distribution coefficients provide an indication of selectivity, capacity, and affinity for a specific ion toward the ion-exchange material.

The ion-exchange selectivity toward alkali and alkaline earth metals for the three compounds, $HK_3(TiO)_{3.5}(GeO)_{0.5}(GeO_4)_{2.5}(SiO_4)_{0.5} \cdot 4H_2O$, $HK_3(TiO)_4(GeO_4)_3 \cdot 4H_2O$, and $HCs_3(TiO)_{3.5}(GeO)_{0.5}(GeO_4)_{2.5}(SiO_4)_{0.5} \cdot 4H_2O$ were determined by batch techniques using 1×10^{-3} M metal ion solutions. For brevity, these compounds will be addressed as KTiSiGe, KTiGe, and CsTiSiGe, respectively.

Examination of Table 10 shows that the potassium Ge-substituted compounds have a low affinity (K_d <100 mL/g) for the alkali cations except for cesium. In fact, these cesium K_ds are much larger than what we presented in our earlier paper for the potassium (K_d = 5800 mL/g), acid (11 000 mL/g), and sodium (15 360 mL/g) forms of the pure titanosilicate pharmacosiderite.[1,2] As we hypothesized, the affinity for cesium increases with an increasing Ge content substituted into the framework structure. To further verify this cesium selectivity, K_d values for CsTiSiGe were also obtained for the alkali and alkaline earth cations. As noted in Table 10, the cesium phase has little affinity for any alkali or alkaline earth cations as indicated by its low K_d values. Again, this high cesium selectivity is reinforced by the very low K_ds for the alkali metals on the cesium phase of the exchanger. Rationalization for the observed selectivity series can be given in terms of structure and will be further addressed in the Discussion section.

Table 10. Distribution Coefficients, K_ds, and Equilibrium pHs (in Parentheses) for the Alkali and Alkaline Earth Metals Using $HK_3(TiO)_{3.5}(GeO)_{0.5}(GeO_4)_{2.5}(SiO_4)_{0.5} \cdot 4H_2O$ (KTiSiGe), $HCs_3(TiO)_{3.5}(GeO)_{0.5}(GeO_4)_{2.5}(SiO_4)_{0.5} \cdot 4H_2O$ (CsTiSiGe), $HK_3(TiO)_4(SiO_4)_3 \cdot 4H_2O$ (KTiSi), and $HK_3(TiO)_4(GeO_4)_3 \cdot 4H_2O$ (KTiGe)

sample	Li	Na	Cs	Mg	Ca	Sr	Ba
KTiSiGe	120	280	32000	4900	5480	7900	72700
	(8.4)	(9.3)	(9.3)	(8.1)	(8.2)	(7.8)	(7.9)
CsTiSiGe	10	90	n/a	100	100	680	280
	(8.9)	(7.9)		(8.3)	(7.7)	(7.6)	(7.3)
KTiGe	200	100	46200	6100	>6990	≫100000	>100000
	(8.5)	(8.2)	(8.5)	(8.2)	(8.3)	(7.2)	(7.3)
KTiSi	750	220	5800	31000	12000	>52000	3100
	(10.1)	(10.7)	(9.7)	(10.6)	(10.7)	(9.6)	(9.4)

A similar selectivity series was observed for the Ge-substituted compounds as compared to their parent potassium titanosilicate; however, KTiGe and KTiSiGe have lower magnesium and calcium K_ds while the strontium and barium values have significantly increased. An explanation for this decrease in calcium and magnesium K_d values can be explained in terms pH, as indicated by the difference in equilibrium pH values for the pure potassium titanosilicate and the Ge-substituted compounds. For example, final solution pHs for calcium and magnesium using the potassium titano-

silicate as an exchanger were 10.6 and 10.7, respectively. Conversely, KTiGe and KTiSiGe produced equilibrium pH values in the range 8.1−8.3. Obviously at higher pHs, most of the magnesium and some of the calcium will precipitate as insoluble metal hydroxides, so the resulting K_d values will exhibit an apparent increase. Another interesting point is the 2-fold increase in strontium K_ds at lower equilibrium pHs for both KTiGe (≫100 000 mL/g) and KTiSiGe (79 000 mL/g) as compared to their parent titanium silicate exchanger (>52 000 mL/g). Likewise, the barium K_ds increase 10-fold from ∼3000 mL/g for the potassium titanosilicate to 72 670 and >100 000 mL/g for KTiSiGe and KTiGe, respectively. A dramatic increase in selectivity for strontium and cesium proves beneficial, especially for specific nuclear waste remediation applications where there is ppm−ppb levels of cesium and strontium admixed with 5−6 M Na^+, 0.4−0.5 M Al, 0.1 M K^+, actinides, and other small concentrations of alkali, alkaline earth, and transition metals.

Discussion

Eisenman[23] enunciated some guiding principles to help in understanding selectivity in glass electrodes as ion exchangers. If the fixed grouping within the exchanger is anionic with radius r_{f^-}, then the electrostatic energy arising from its interaction with a cation A^+ with a radius r_{A^+} is $e^2/(r_{f^+} + r_{A^+})$, where e is the electron charge. The interaction of the fixed grouping with cation B^+ gives rise to a similar term. Thus, for the exchange reaction 1

$$\overline{RA}^+ + B^+(g) \leftrightarrows \overline{RB}^+ + A^+(g) \qquad (1)$$

where the barred entities represent the solid-phase exchanger and the ions are unhydrated, the change in free energy for reaction R1 is then

$$\Delta G_E^\circ = \frac{e^2}{r_{f^-} + r_{A^+}} - \frac{e^2}{r_{f^-} + r_{B^+}} \qquad (2)$$

If the ingoing ion (B^+) approaches the negative site more closely than the outgoing cation (A^+), then the free energy will be negative. On this basis, we might expect cesium cations to be the least tightly coordinated while protons would be the highest. However, there are two factors that counter the electrostatic effect as stated by Eisenman. In this case, exchange takes place in aqueous media so the change in ion hydration also needs to be considered. Eisenman assumed that the ions (A^+) within the glass were unhydrated and, upon entering the solution, they would undergo a free energy change that was equivalent to the free energy of hydration for the individual ions, $-\Delta G_{A^+}$. Upon entering the exchanger, ion B^+ would need to release its hydration shell with a free energy change, $+\Delta G_{B^+}$. For this example, the exchanger's water content remains constant no matter which ion (except H^+) is present. Thus, the differences in hydration energies require modification in order to account for partial hydration (e.g., Li^+) to a fully hydrated state (e.g., Cs^+).

(23) Eisenman, G. *Biophys. J. Suppl.* **1962**, *2*, 259.

Table 11. Average Bond Lengths (Å) and Bond Ratios of Alkali Metals in the Pharmacosiderite Phases[a]

alkali metal ion (M^+)	average bond distances (Å) and (normalized value)		
	MTiSi	MTiSiGe	MTiGe
K^+	3.213 (1.09)	(1.13)	(1.20)
		3.186 (1.07)	3.134 (1.06)
Cs^+	3.258 (1.00)	3.306 (1.02)	(1.04)
			(1.01)
			(1.04)
			3.282 (1.04)

[a] MTiSi: $HM_3(TiO)_4(SiO_4)_3 \cdot 4H_2O$. MTiSiGe: $HM_3(TiO)_{3.5}(GeO)_{0.5}(GeO_4)_{2.5}(SiO_4)_{0.5} \cdot 4H_2O$. MTiGe: $HM_3(TiO)_4(GeO_4)_3 \cdot 4H_2O$.

The second consideration involves replacing the $r_{f^-} + r_{M^+}$ term in eq 2 with an expression that contains all bond formations in the coordination sphere of ions B^+ within the exchanger. As a criterion for bond strength, we can use a normalization factor that involves summing the two ionic radii, which represents their strongest bond, assign this value as 1.00, and divide the observed bond distance by the sum of the ionic radii to yield the normalized value. On the basis of this principle, bonds at larger distances than this sum are considered weaker and would have higher normalized values. Table 11 presents average bond length data and their respective normalized values (in parentheses) for alkali cations and O^{2-}. The bond length values were calculated as a sum of the ionic radii, $r_{M^+} + r_{O^{2-}}$, where M^+ is the alkali metal under consideration and O^{2-} represents the silicate/germanate framework oxygen. For example, the average K−O interatomic distance in the compound $HK_3(TiO)_4(GeO_4)_3 \cdot 4H_2O$ is 3.213 Å. Dividing this value by the sum of ionic radii for K^+ and O^{2-} (with identical coordination numbers)[24] gives 1.09, the value in parentheses. To determine whether the selectivity for a particular ion is greater or less than that for another ion by one of the phases listed, for example, cesium over potassium, it is also necessary to divide the normalized values.

For the phase $HM_3(TiO)_4(SiO_4)_3 \cdot 4H_2O$ ($M^+ = K^+$, Cs^+), the ratio of normalized bond values (K^+/Cs^+) is 1.09, and for compound $HM_3(TiO)_{3.5}(GeO)_{0.5}(GeO_4)_{2.5}(SiO_4)_{0.5} \cdot 4H_2O$, the value is 1.11. As this ratio increases, the phase becomes more selective toward cesium. That is, a lower bond strength will have a higher normalized value. Thus, a high bond strength for cesium (low normalized value) divided into a large value for potassium, will result in a high ratio. According to this reasoning, cesium selectivity should be greater in $HM_3(TiO)_{3.5}(GeO)_{0.5}(GeO_4)_{2.5}(SiO_4)_{0.5} \cdot 4H_2O$ (KTiSiGe) as opposed to its parent titanium silicate structure, $HM_3(TiO)_4(SiO_4)_3 \cdot 4H_2O$ (KTiSi). Examination of Table 10 supports our logic because the cesium K_d value for KTiSiGe (32 000 mL/g) is much higher than that for KTiSi (5800 mL/g).

In the case of multiple ion sites, like those in compounds $HK_3(TiO)_4(GeO_4)_3 \cdot 4H_2O$ and $HK_3(TiO)_{3.5}(GeO)_{0.5}(GeO_4)_{2.5}(SiO_4)_{0.5} \cdot 4H_2O$, we would expect that the potassium ion with the weakest bonds would exchange first and a cesium ion would subsequently occupy the most favorable site. The high bond ratio in this phase corresponds to 1.20/1.01 or 1.19, so this phase

(24) Prewitt, C. T.; Shannon, R. D. *Trans. Am. Crystallogr. Assoc.* **1969**, *5*, 57.

is the most selective for cesium, producing a K_d of 46 200 mL/g. However, one cannot overlook the possibility that the ions may rearrange during exchange. In the case of $HM_3(TiO)_4(GeO_4)_3 \cdot 4H_2O$, the average normalized value for cesium is 1.03, which gives a ratio of 1.16. We choose the higher value for potassium, 1.20, because it is very unlikely that a strongly held potassium ion would exchange first. However, this point requires additional justification by carrying out Rietveld refinements for partially exchanged potassium and cesium phases. The ideas governing selectivity are not limited to the pharmacosiderite-type ion exchangers but, in fact, the same principles need to be applied to other tight tunnel structures.

Last, the discussion presented in this paper focused primarily on cesium selectivity that was related to cesium−oxygen bond strengths. However, we cannot overlook the fact that strontium uptake in aqueous solution also increased with the amount of germanium that substituted into the framework structure. We are currently attempting to solve the structure for a crystalline, fully substituted strontium titanosilicate pharmacosiderite using powder X-ray diffraction and Rietveld methods. This study should provide us with greater insight into the relationship between structure and strontium selectivity.

Acknowledgment. Funding was provided by the U.S. Department of Energy, Grant No. 198567-A-F1, through Pacific Northwest National Laboratory under the DOE's Office of Science and Technology's Efficient Separations and Processing Crosscutting Program and the DOE Basic Energy Sciences, Grant No. 434741-00001, funded by the Environmental Management Office. E.A.B. thanks Dr. Franz Gingl and Dr. Jay (Cahit) Eylem for their assistance and discussions regarding crystallographic data.

CM970037R